PERGAMON

International Journal of Solids and Structures 39 (2002) 585–600

INTERNATIONAL JOURNAL OF SOLIDS and STRUCTURES

www.elsevier.com/locate/ijsolstr

Nonlinear behaviour of interacting dielectric cracks in piezoelectric materials

X.D. Wang *, L.Y. Jiang

Department of Mechanical Engineering, University of Alberta, 4–9 Mechanical Engineering Building, Edmonton, Alberta, Canada T6G 2G8

Received 16 January 2001

Abstract

Existing studies on the fracture of cracked piezoelectric materials have been limited mostly to the electrically impermeable and permeable crack models, which represent the limiting cases of the physical boundary condition along the crack surfaces. This paper presents a study on the electromechanical behaviour of interacting dielectric cracks in piezoelectric materials. The cracks are filled with dielectric media and, as the result, the electric boundary condition along the crack surfaces is governed by the opening displacement of the cracks. The formulation of this nonlinear problem is based on simulating the cracks using distributed dislocations and solving the resulting nonlinear singular integral equations. Multiple deformation modes are observed. A solution technique is developed to determine the desired deformation mode of the interacting cracks. Numerical results are given to show the effect of the interaction between parallel cracks. Attention is paid to the transition between permeable and impermeable models with increasing crack opening.

Keywords: Piezoelectricity; Dielectric cracks; Electromechanical coupling; Interacting cracks; Deformation-dependent boundary conditions

1. Introduction

Because of their coupling nature between mechanical and electric fields, piezoelectric materials have been widely used in electromechanical devices, such as actuators, sensors and transducers. The newly developed piezoceramic materials with stronger piezoelectric effects are generally brittle and have a tendency to develop multiple cracks during manufacturing and service processes. As the result, the evaluation of the coupling between mechanical and electric fields and its effect upon the fracture behavior of this type of piezoelectric materials are of great importance and have drawn significant attention from the research communities.

Unlike traditional crack problems where the crack surface boundary condition is well defined, the electric boundary condition along crack surfaces in piezoelectric materials is still one of the fundamental issues requiring further studies. There are two typical crack models using different electric boundary

* Corresponding author. Fax: +1-780-492-2200.
E-mail address: xiaodong.wang@ualberta.ca (X.D. Wang).

0020-7683/02/$ - see front matter
PII: S0020-7683(01)00199-8

conditions. One is the electrically permeable model proposed by Parton (1976), which has been used in studying both the static and dynamic fracture behavior of piezoelectric materials (Wang, 2000). Another one is the impermeable model, which has been extensively used to study the fracture of piezoelectric materials (e.g., see, Deeg, 1980; Pak, 1990; Suo et al., 1992; Pak, 1992; Park and Sun, 1995). These models represent two limiting cases where the electric permittivity of the crack is assumed to be infinite and zero, respectively. To determine the effect of the dielectric medium inside a crack upon the electric boundary condition, an elliptical crack model (see, McMeeking, 1989; Sosa, 1991; Dunn, 1994; Zhang and Tong, 1996; Zhang et al., 1998) has been used to study the effect of crack opening. Their results indicate that the permeable condition may underestimate the effect of the electric field on the crack propagation and the impermeable model may overestimate its effect. It should be mentioned that this elliptical crack model represents only the effect of the initial crack opening. For a slit crack, since the dielectric constant of piezoceramic is much higher than that of the air (or vacuum) filling the crack, the electric boundary condition may be very sensitive to the crack opening caused by the applied mechanical and electric loads. In this case, the crack can be modelled as a dielectric crack filled with a dielectric medium.

Because of the brittleness of piezoceramic materials, the interaction between multiple cracks may significantly affect their fracture property. Although the interaction between cracks in traditional brittle materials have been extensively studied (e.g., see, Rubinstein, 1986; Chudnovsky et al., 1987; Gong and Meguid, 1991; Chen and Hasebe, 1994; Meguid and Wang, 1995), relatively fewer studies have been conducted to deal with the interacting effect of multiple cracks in piezoelectric materials (see, Han and Wang, 1999; Chen and Han, 1999a,b). No attempt has been made in determining the effect of interaction between dielectric cracks, for which the electric boundary condition depends on the crack opening.

It is therefore the objective of the current paper to provide a theoretical study of the nonlinear electromechanical behaviour of interacting dielectric cracks. Based on the use of the dislocation model of the cracks and the solution of the resulting nonlinear singular integral equations, numerical simulation is conducted to study the effect of the dielectric medium filling the crack and the crack interaction upon the fracture behaviour of the cracked medium. Special attention is paid to the transition between permeable and impermeable crack models with increasing crack opening.

2. Formulation of the problem

The problem envisaged is a generalized plane problem of N interacting parallel cracks in an infinite piezoelectric medium, as shown in Fig. 1 with the centre of the kth crack being located at (X_k, Y_k) in the global coordinate system oxy. Local Cartesian coordinate systems (x_k, y_k) $(k = 1, 2, \ldots, N)$ are used to describe the cracks, with crack k lying along x_k and the origin of (x_k, y_k) being the centre of the crack. The piezoelectric medium is assumed to be transversely isotropic with the so-called poling direction being perpendicular to the crack surfaces. The cracked medium is subjected to a stress field σ_{2i}^{∞} $(i = 1, 2, 3)$, with 1, 2, 3 corresponding to x, y and z, respectively. The applied electric loading at infinity is the electric displacement D_2^{∞}. The cracks are assumed to be filled with a dielectric medium with negligible elastic constants (air or vacuum).

In the absence of free charges and body forces, the electromechanical behaviour of a piezoelectric medium is governed by the equilibrium equation and the Gauss law,

$$\sigma_{ij,j} = 0; \quad D_{i,i} = 0 \tag{1}$$

and the constitutive equations,

$$\sigma_{ij} = c_{ijrs}\varepsilon_{rs} - e_{rij}E_r; \qquad D_i = e_{irs}\varepsilon_{rs} + \epsilon_{ij}E_j \tag{2}$$

where c_{ijrs}, e_{irs} and ϵ_{ij} are elastic, piezoelectric and dielectric constants, respectively, $i, j, r, s = 1, 2, 3$, with 1, 2, 3 corresponding to x, y and z, respectively. ε_{rs} and E_r are strain and electric field intensity defined by

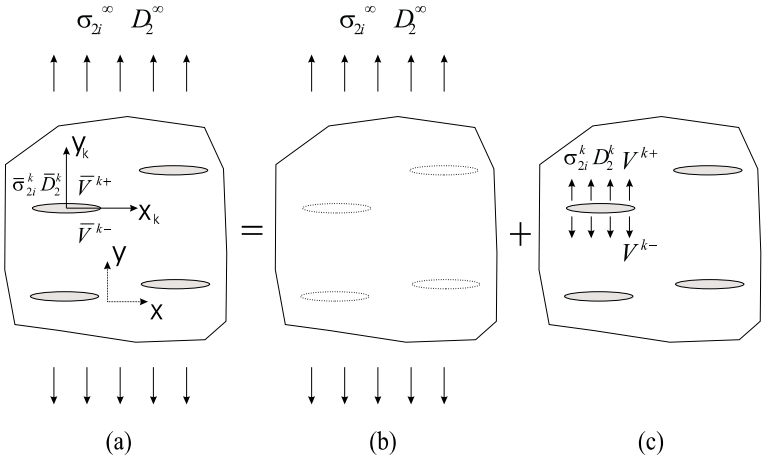

Fig. 1. Crack model and the decomposition of the problem.

$$\varepsilon_{rs} = \frac{1}{2}\left(\frac{\partial u_r}{\partial x_s} + \frac{\partial u_s}{\partial x_r}\right); \qquad E_r = -\frac{\partial V}{\partial x_r} \tag{3}$$

with u_r and V being the displacement and the electric potential. For the generalized plane problem considered, it is assumed that u_r and V depend only on in-plane coordinates, i.e. $u_r = u_r(x, y)$, $r = 1, 2, 3$ and $V = V(x, y)$. Substituting Eqs. (2) and (3) into Eq. (1) results in the following governing equation of the problem,

$$(\mathbf{Q}X^2 + (\mathbf{R} + \mathbf{R}^{\mathrm{T}})XY + \mathbf{T}Y^2)\mathbf{v} = 0 \tag{4}$$

where $X = \partial/\partial x$, $Y = \partial/\partial y$, and

$$\mathbf{v}^{\mathrm{T}} = \{u_1, u_2, u_3, V\} \tag{5}$$

$$\mathbf{Q} = \begin{bmatrix} c_{11} & c_{16} & c_{15} & e_{11} \\ c_{61} & c_{66} & c_{65} & e_{16} \\ c_{15} & c_{65} & c_{55} & e_{15} \\ e_{11} & e_{16} & e_{15} & -\epsilon_{11} \end{bmatrix}$$

$$\mathbf{R} = \begin{bmatrix} c_{16} & c_{12} & c_{14} & e_{21} \\ c_{66} & c_{26} & c_{25} & e_{26} \\ c_{56} & c_{46} & c_{54} & e_{25} \\ e_{16} & e_{12} & e_{14} & -\epsilon_{12} \end{bmatrix}$$

$$\mathbf{T} = \begin{bmatrix} c_{66} & c_{62} & c_{64} & e_{26} \\ c_{26} & c_{22} & c_{24} & e_{22} \\ c_{46} & c_{42} & c_{44} & e_{24} \\ e_{26} & e_{22} & e_{24} & -\epsilon_{22} \end{bmatrix}$$

The elements in **Q**, **R**, **T** are material constants in matrix notations. In the following discussions, bold letters will be used to represent matrices and/or vectors.

Similar to the traditional crack model, the crack surfaces are traction free, i.e. for crack k, following conditions should be satisfied in the local coordinate system,

$$\overline{\sigma}_{2i}^{k}(x_k, 0) = 0 \tag{6}$$

where $i = 1, 2, 3$ with 1, 2, 3 corresponding to x_k, y_k and z_k, respectively.

Since the dielectric constants of typical piezoelectric materials are 10^3 times higher than that of the air (or vacuum) filling the crack, the electric boundary condition along the crack surfaces may be sensitive to the opening deformation of the crack. To evaluate this effect, the deformed geometry of the crack will be used in the formulation of the problem. Accordingly, the electric boundary condition along the surfaces of crack k is,

$$\overline{D}_2^k = -\epsilon_0 \frac{\overline{V}^{k+} - \overline{V}^{k-}}{d_2^k} \tag{7}$$

where $d_2^k = u_2^{k+} - u_2^{k-}$ is the opening deformation for crack k, and $\epsilon_0 = 8.85 \times 10^{-12}$ C/V m is the dielectric constant of air inside the crack.

3. Fundamental solution for a single dislocation

Although the use of dielectric crack model will induce nonlinear deformation, the nonlinearity will be limited only to the crack boundary conditions. The interacting cracks can be modelled as the superposition of distributed dislocations (or jumps of displacements and electric potentials across the crack surfaces).

Consider a dislocation defined by,

$$\mathbf{d}(x) = \mathbf{v}^+ - \mathbf{v}^- = \mathbf{d}_0 H(x), \tag{8}$$

with $\mathbf{v}^+$ and $\mathbf{v}^-$ representing the displacement and electric potential along upper and lower surfaces of the crack as defined in Eq. (5), $\mathbf{d}_0$ being a constant vector and $H(x)$ being the Heaviside step function.

Eq. (4) can be solved using Fourier transform with respect to x, which yields

$$-s^2\mathbf{Q}\mathbf{v}^* - \mathrm{i}s(\mathbf{R} + \mathbf{R}^{\mathrm{T}})\frac{\partial \mathbf{v}^*}{\partial y} + \mathbf{T}\frac{\partial^2 \mathbf{v}^*}{\partial y^2} = 0$$

with superscript '$*$' representing Fourier transform. The solution of $\mathbf{v}^*$ is generally in the form of

$$\mathbf{v}^* = \mathbf{a}\,\mathrm{e}^{-\mathrm{i}\eta y} \tag{9}$$

where $\mathbf{a}$ and η can be determined by solving the following eigenvalue problem

$$[\mathbf{Q} + p(\mathbf{R} + \mathbf{R}^{\mathrm{T}}) + p^2\mathbf{T}]\mathbf{a} = 0 \tag{10}$$

with $p = \eta/s$. It has been proved that this equation has no real roots (Suo et al., 1992). Let p_α be the eigenvalues with positive imaginary parts, $\mathbf{a}_\alpha$ the corresponding eigenvectors, and $\bar{p}_\alpha$ and $\bar{\mathbf{a}}_\alpha$ the conjugates of p_α and $\mathbf{a}_\alpha$, which are also the eigenvalues and eigenvectors of Eq. (10). To build a solution which vanishes at infinity, define $\eta_\alpha = p_\alpha s$, $\bar{\eta}_\alpha = \bar{p}_\alpha s$ for $s > 0$ and $\eta_\alpha = \bar{p}_\alpha s$, $\bar{\eta}_\alpha = p_\alpha s$ for $s < 0$. The general solution of $\mathbf{v}^*$ can then be expressed in terms of a linear combination of solutions given by Eq. (9) for different eigenvalues, such that

$$\mathbf{v}^* = (\mathbf{A}\mathbf{F}\mathbf{f}^r + \overline{\mathbf{A}}\mathbf{F}'\mathbf{g}^r)H(s) + (\overline{\mathbf{A}}\mathbf{F}\mathbf{f}^l + \mathbf{A}\mathbf{F}'\mathbf{g}^l)H(-s) \tag{11}$$

where $\mathbf{A} = [\mathbf{a}_1, \mathbf{a}_2, \mathbf{a}_3, \mathbf{a}_4]$ and $\overline{\mathbf{A}} = [\bar{\mathbf{a}}_1, \bar{\mathbf{a}}_2, \bar{\mathbf{a}}_3, \bar{\mathbf{a}}_4]$ are known matrices determined by the eigenvectors. The matrices $\mathbf{F}$ and $\mathbf{F}'$ are given by

$$\mathbf{F}(s, y) = \mathrm{diag}[\mathrm{e}^{-\mathrm{i}\eta_1 y}, \mathrm{e}^{-\mathrm{i}\eta_2 y}, \mathrm{e}^{-\mathrm{i}\eta_3 y}, \mathrm{e}^{-\mathrm{i}\eta_4 y}] \tag{12}$$

$$\mathbf{F}'(s, y) = \mathrm{diag}[\mathrm{e}^{-\mathrm{i}\bar{\eta}_1 y}, \mathrm{e}^{-\mathrm{i}\bar{\eta}_2 y}, \mathrm{e}^{-\mathrm{i}\bar{\eta}_3 y}, \mathrm{e}^{-\mathrm{i}\bar{\eta}_4 y}]. \tag{13}$$

f and **g** are coefficient vectors to be determined with the superscripts r and l representing the right ($s > 0$) and left ($s < 0$) half planes. The corresponding stress and electric displacement fields can be expressed as,

$$\mathbf{t} = \mathbf{R}^{\mathrm{T}} \frac{\partial \mathbf{v}}{\partial x} + \mathbf{T} \frac{\partial \mathbf{v}}{\partial x} \tag{14}$$

with $\mathbf{t}^{\mathrm{T}} = \{\sigma_{21}, \sigma_{22}, \sigma_{23}, D_2\}$.

Applying Fourier transform with respect to x to Eq. (14) and using Eq. (11), the Fourier transform of **t** is obtained,

$$\mathbf{t}^* = -\mathrm{i}s(\mathbf{B}\mathbf{F}\mathbf{f}^r + \overline{\mathbf{B}}\mathbf{F}'\mathbf{g}^r)H(s) - \mathrm{i}s(\overline{\mathbf{B}}\mathbf{F}\mathbf{f}^l + \mathbf{B}\mathbf{F}'\mathbf{g}^l)H(-s) \tag{15}$$

where the matrix **B** is given by

$$\mathbf{B} = \mathbf{R}^{\mathrm{T}}\mathbf{A} + \mathbf{T}\mathbf{A}\mathbf{P} \tag{16}$$

with $\mathbf{P} = \mathrm{diag}[p_1,\ p_2,\ p_3,\ p_4]$.

The general solution of **v** and **t** can then be obtained using the inverse Fourier transform of Eqs. (11) and (15) as

$$\mathbf{v}(x,y) = \int_0^\infty (\mathbf{A}\mathbf{F}\mathbf{f}^r + \overline{\mathbf{A}}\mathbf{F}'\mathbf{g}^r)\mathrm{e}^{-\mathrm{i}sx}\,\mathrm{d}s + \int_{-\infty}^0 (\overline{\mathbf{A}}\mathbf{F}\mathbf{f}^l + \mathbf{A}\mathbf{F}'\mathbf{g}^l)\mathrm{e}^{-\mathrm{i}sx}\,\mathrm{d}s \tag{17}$$

$$\mathbf{t}(x,y) = -\mathrm{i}\int_0^\infty s(\mathbf{B}\mathbf{F}\mathbf{f}^r + \overline{\mathbf{B}}\mathbf{F}'\mathbf{g}^r)\mathrm{e}^{-\mathrm{i}sx}\,\mathrm{d}s - \mathrm{i}\int_{-\infty}^0 s(\overline{\mathbf{B}}\mathbf{F}\mathbf{f}^l + \mathbf{B}\mathbf{F}'\mathbf{g}^l)\mathrm{e}^{-\mathrm{i}sx}\,\mathrm{d}s \tag{18}$$

From Eqs. (12), (13) and (18), it can be observed that $\mathbf{f}^r = 0$, $\mathbf{f}^l = 0$ for $y > 0$, while $\mathbf{g}^r = 0$, $\mathbf{g}^l = 0$ for $y < 0$ to ensure that **t** is bounded at infinity.

At $y = 0$, **F** and $\mathbf{F}'$ become the unit matrix **I**, and the continuity of **t** along the x axis ($\mathbf{t}^+ = \mathbf{t}^-$) will result in $\overline{\mathbf{B}}\mathbf{g}^r = \mathbf{B}\mathbf{f}^r$, $\mathbf{B}\mathbf{g}^l = \overline{\mathbf{B}}\mathbf{f}^l$. From Eq. (11), the displacement and electric potential difference between the upper and lower surfaces of the crack is

$$\mathbf{v}^{*+} - \mathbf{v}^{*-} = \mathrm{i}\mathbf{H}(\mathbf{B}\mathbf{f}^r H(s) - \overline{\mathbf{B}}\mathbf{f}^l H(-s)) \tag{19}$$

where

$$\mathbf{H} = -2\,\mathrm{Im}(\mathbf{A}\mathbf{B}^{-1}) \tag{20}$$

H is symmetric and only the last element h_{44} is negative (Suo et al., 1992). For a dislocation defined by Eq. (8), the Fourier transform of the jump of **v** across the crack surfaces can be determined, such that

$$\mathbf{v}^{*+} - \mathbf{v}^{*-} = -\frac{1}{2\pi}\frac{\mathbf{d}_0}{\mathrm{i}s} \tag{21}$$

Substituting Eq. (21) into Eq. (19) gives

$$\begin{aligned} \mathbf{H}\mathbf{B}\mathbf{f}^r &= \frac{\mathbf{d}_0}{2\pi s}, \quad s > 0 \\ \mathbf{H}\overline{\mathbf{B}}\mathbf{f}^l &= -\frac{\mathbf{d}_0}{2\pi s}, \quad s < 0 \end{aligned} \tag{22}$$

The Fourier transform of the stress and electric displacement fields due to a dislocation given by Eq. (8) can then be obtained using Eqs. (15) and (22), as

$$\mathbf{t}^* = -\mathrm{i}\mathbf{H}^{-1}\frac{\mathbf{d}_0}{2\pi}\mathrm{sgn}(s) \quad (y = 0) \tag{23}$$

$$\mathbf{t}^{*+} = -\mathrm{i}(\overline{\mathbf{B}}\mathbf{F}'\overline{\mathbf{B}}^{-1}\mathbf{H}^{-1})\frac{\mathbf{d}_0}{2\pi}\mathbf{H}(s) + \mathrm{i}(\mathbf{B}\mathbf{F}'\mathbf{B}^{-1}\mathbf{H}^{-1})\frac{\mathbf{d}_0}{2\pi}\mathbf{H}(-s) \quad (y > 0) \tag{24}$$

$$\mathbf{t}^{*-} = -\mathrm{i}(\mathbf{B}\mathbf{F}\mathbf{B}^{-1}\mathbf{H}^{-1})\frac{\mathbf{d}_0}{2\pi}\mathbf{H}(s) + \mathrm{i}(\overline{\mathbf{B}}\mathbf{F}\overline{\mathbf{B}}^{-1}\mathbf{H}^{-1})\frac{\mathbf{d}_0}{2\pi}\mathbf{H}(-s) \quad (y < 0) \tag{25}$$

The stress and electric displacement fields can be obtained using the inverse Fourier transform of Eqs. (23)–(25) as

$$\mathbf{t}(x,y) = -\left[\mathbf{B}_1\left(\frac{1}{x+p_iy}\right) + \mathbf{B}_2\left(\frac{1}{x+\bar{p}_iy}\right)\right]\mathbf{H}^{-1}\mathbf{d}_0 \tag{26}$$

where

$$\mathbf{B}_1\left(\frac{1}{x+p_iy}\right) = \mathrm{i}\frac{1}{2\pi}\int_0^\infty \mathbf{B}\mathbf{F}\mathbf{B}^{-1}\,\mathrm{e}^{-\mathrm{i}sx}H(s)\,\mathrm{d}s \tag{27}$$

$$\mathbf{B}_2\left(\frac{1}{x+\bar{p}_iy}\right) = \mathrm{i}\frac{1}{2\pi}\int_0^\infty \overline{\mathbf{B}}\mathbf{F}'\overline{\mathbf{B}}^{-1}\,\mathrm{e}^{-\mathrm{i}sx}H(s)\,\mathrm{d}s \tag{28}$$

4. Interacting dielectric cracks

Consider now the interaction between multiple cracks shown in Fig. 1. This problem can be decomposed into two subproblems (b) and (c) with problem (b) containing only the homogeneous medium without any cracks, and problem (c) being concerned with the multiple cracks subjected to external loads along the deformed crack surfaces. The interacting cracks in subproblem (c) can be generally simulated using distributed dislocations along the crack lines. By superimposing the single dislocation solution given by Eq. (26), the stress and electric displacement fields caused by the kth crack can be expressed in the local coordinate system (x_k, y_k) as,

$$\mathbf{t}(x_k,y_k) = -\int_{-a_k}^{a_k}\left[\mathbf{B}_1\left(\frac{1}{(x_k+p_iy_k)-\xi}\right) + \mathbf{B}_2\left(\frac{1}{(x_k+\bar{p}_iy_k)-\xi}\right)\right]\mathbf{\Gamma}^{k'}(\xi)\,\mathrm{d}\xi \tag{29}$$

where $2a_k$ is the crack length and $\mathbf{\Gamma}^k = \mathbf{H}^{-1}\mathbf{d}^k$ with $\mathbf{d}^k(x) = \mathbf{v}^{k+}(x,0) - \mathbf{v}^{k-}(x,0)$. The superscripts '+' and '−' represent the upper and lower surfaces of the cracks, respectively. The stress and electric displacement fields caused by kth crack at the location of lth crack can be expressed in the local coordinate system (x_l, y_l) as,

$$\mathbf{t}^{lk}(x_l,y_l) = \int_{-a_k}^{a_k}\left[\mathbf{B}_1\left(\frac{1}{\xi-(x_l+x_{lk}+p_iy_{lk})}\right) + \mathbf{B}_2\left(\frac{1}{\xi-(x_l+x_{lk}+\bar{p}_iy_{lk})}\right)\right]\mathbf{\Gamma}^{k'}(\xi)\,\mathrm{d}\xi \tag{30}$$

where $x_{lk} = X_l - X_k$ and $y_{lk} = Y_l - Y_k$.

In problem (c) of Fig. 1, according to the deformed geometry, each crack should satisfy the following boundary conditions, which are consistent with the original boundary conditions (6) and (7),

$$\sigma_{2i}^{k+} = \sigma_{2i}^{k-} = -\sigma_{2i}^{\infty} \tag{31}$$

$$D_2^{k+} = D_2^{k-} = D_2^k; \qquad D_2^k + D_2^\infty + \frac{\epsilon_0}{d_2^k}(V^{k+} - V^{k-}) + \epsilon_0 E_2^\infty = 0 \tag{32}$$

where E_2 is the applied electric field intensity. Since the dielectric constants of piezoceramic materials are typically 10^3 times higher than ϵ_0, the additional term $\epsilon_0 E_2^\infty$ can be ignored in comparison with D_2^∞. The boundary conditions (31) and (32) can be written in a matrix form as,

$$\sum_{k=1}^{N} \mathbf{t}^{lk} + \mathbf{t}^0 + \mathbf{K}^l(\mathbf{v}^{l+} - \mathbf{v}^{l-}) = 0 \quad (l = 1, 2, \ldots, N) \tag{33}$$

where $\mathbf{t}^0 = \{\sigma_{21}^\infty, \sigma_{22}^\infty, \sigma_{23}^\infty, D_2^\infty\}^{\mathrm{T}}$ and the only nonvanishing elements of matrices $\mathbf{K}^l$ is $k_{44}^l = \epsilon_0/d_2^l$.

Substituting Eq. (30) into the general boundary conditions (33), the following nonlinear singular integral equations can be obtained,

$$\frac{1}{\pi}\int_{-a_l}^{a_l} \frac{\mathbf{\Gamma}^{l'}(\xi)}{\xi - x_l}\,\mathrm{d}\xi + \sum_{k\neq l}^{N}\left(\int_{-a_k}^{a_k}\left[\mathbf{B}_1\left(\frac{1}{\xi - (x_l + x_{lk} + p_i y_{lk})}\right) + \mathbf{B}_2\left(\frac{1}{\xi - (x_l + x_{lk} + \bar{p}_i y_{lk})}\right)\right]\mathbf{\Gamma}^{k'}(\xi)\,\mathrm{d}\xi\right) + \mathbf{t}^0 + \mathbf{K}^l\mathbf{H}\mathbf{\Gamma}^l(x_l) = 0 \quad (l = 1, 2, \ldots, N) \tag{34}$$

The integral equations given in Eq. (34) are characterized by square root singularity and, therefore, the general solution of them can be expressed as,

$$\mathbf{\Gamma}^{l'}(\xi) = \sum_{m=1}^{\infty} \mathbf{C}_m^l T_m\left(\frac{\xi}{a_l}\right) \Bigg/ \sqrt{1 - \frac{\xi^2}{a_l^2}} \tag{35}$$

where $\mathbf{C}_m^l = \{c_{1m}^l, c_{2m}^l, c_{3m}^l, c_{4m}^l\}^{\mathrm{T}}$ are unknown vectors to be determined and $T_m(\xi/a_l)$ are the first kind of Chebyshev polynomials of the mth order.

Substituting Eq. (35) into Eq. (34), the following nonlinear algebraic equations can be obtained,

$$\sum_{m=1}^{\infty} \mathbf{C}_m^l \frac{\sin\left(m\cos^{-1}\frac{x_l}{a_l}\right)}{\sin\left(\cos^{-1}\frac{x_l}{a_l}\right)} + \sum_{k\neq l}^{N}\sum_{m=1}^{\infty}\int_{-a_k}^{a_k}(\mathbf{B}_1 + \mathbf{B}_2)\mathbf{C}_m^k T_m\left(\frac{\xi}{a_k}\right)\Bigg/\sqrt{1 - \left(\frac{\xi}{a_k}\right)^2}\,\mathrm{d}\xi - \sum_{m=1}^{\infty}\mathbf{M}^l\mathbf{C}_m^l\frac{a_l}{m}\sin\left(m\cos^{-1}\frac{x_l}{a_l}\right) = -\mathbf{t}^0 \quad (l = 1, 2, \ldots, N) \tag{36}$$

where

$$\mathbf{M}^l = \begin{bmatrix} 0 & 0 & 0 & 0 \\ 0 & 0 & 0 & 0 \\ 0 & 0 & 0 & 0 \\ h_{41}\frac{\epsilon_0}{d_2^l} & h_{42}\frac{\epsilon_0}{d_2^l} & h_{43}\frac{\epsilon_0}{d_2^l} & h_{44}\frac{\epsilon_0}{d_2^l} \end{bmatrix} \tag{37}$$

$$d_2^l = -\sum_{m=1}^{\infty}[h_{21}c_{1m}^l + h_{22}c_{2m}^l + h_{23}c_{3m}^l + h_{24}c_{4m}^l]\frac{a_l}{m}\sin\left(m\cos^{-1}\frac{x_l}{a_l}\right) \tag{38}$$

The unknown parameters $\mathbf{C}_m^l$ can be determined by solving Eq. (36), from which the electromechanical behaviour of the interacting crack can be predicted. The governing equation (36) is assumed to be satisfied, for each crack, at M collocation points $x_n = a_l\cos((n-1)\pi/(M-1))$ $(n = 1, 2, \ldots, M)$ and the Chebyshev polynomials are truncated at Mth term. The governing equations are then reduced to a system of algebraic

equations. The mechanical and electric behaviour of interacting dielectric cracks can be determined by solving these equations.

5. Fracture parameters

The singular stress and electric displacement **t** ahead of the tip of the lth crack can be expressed as,

$$\mathbf{t}^l(x_l) = \frac{\mathbf{k}^l}{\sqrt{2\pi(x_l - a_l)}} \quad (l = 1, 2, \ldots, N) \tag{39}$$

and the jumps of the displacement and electric potential across the crack surfaces are

$$\mathbf{d}^l(x_l) = \sqrt{\frac{2(a_l - x_l)}{\pi}}\mathbf{H}\mathbf{k}^l \quad (l = 1, 2, \ldots, N) \tag{40}$$

where $\mathbf{k}^l = \{K^l_{\mathrm{II}}, K^l_{\mathrm{I}}, K^l_{\mathrm{III}}, K^l_{\mathrm{IV}}\}^{\mathrm{T}}$ with K^l_{I}, K^l_{II}, K^l_{III} and K^l_{IV} being the stress intensity factors and the electric displacement intensity factor, respectively, which are given by

$$\mathbf{k}^l = -\sqrt{\pi a_l}\sum_{m=1}^{M}\mathbf{C}^l_m \quad (l = 1, 2, \ldots, N) \tag{41}$$

It is well known that the usage of energy release rate in predicting the fracture of cracked piezoelectric media has a drawback. Using this fracture criterion, it is predicted that the electric field always impedes the crack propagation, which is in contradict with the existing experimental results (McHenry and Koepke, 1983; Tobin and Pak, 1993 for examples). As mentioned by Park and Sun (1995), total energy release rate may not be a suitable fracture criterion for piezoelectric materials. To describe the mechanical deformation, it is interesting to consider the property of the crack opening displacement (COD). In the current case, a COD intensity factor K_{COD} can be used to describe the opening deformation of the crack surfaces, which is defined by

$$K^l_{\mathrm{COD}} = \lim_{x_l \to a_l}\frac{d^l_2}{\sqrt{a_l - x_l}} = \sqrt{\frac{2}{\pi}}\{h_{21}\ h_{22}\ h_{23}\ h_{24}\}\mathbf{k}^l \quad (l = 1, 2, \ldots, N) \tag{42}$$

and can be determined directly from the results of $\mathbf{k}^l$.

In the following discussions, both $\mathbf{k}^l$ and K_{COD} will be used to describe the fracture behaviour of interacting cracks.

6. Results and discussion

Attention will be focused on the case where the cracked medium is subjected to a tensile mechanical load $\sigma^{\infty}_{22} > 0$ and an electric load D^{∞}_2 (or E^{∞}_2). For such a plane problem, the corresponding **Q**, **R** and **T** are the follows,

$$\mathbf{Q} = \begin{bmatrix} c_{11} & 0 & 0 \\ 0 & c_{33} & e_{31} \\ 0 & e_{31} & -\epsilon_{11} \end{bmatrix}$$

$$\mathbf{R} = \begin{bmatrix} 0 & c_{12} & e_{12} \\ c_{33} & 0 & 0 \\ e_{31} & 0 & 0 \end{bmatrix}$$

$$\mathbf{T} = \begin{bmatrix} c_{33} & 0 & 0 \\ 0 & c_{22} & e_{22} \\ 0 & e_{22} & -\epsilon_{22} \end{bmatrix}$$

with the materials constants being

$$c_{11} = 13.9 \times 10^{10}\ \mathrm{N/m^2}$$

$$c_{12} = 7.43 \times 10^{10}\ \mathrm{N/m^2}$$

$$c_{22} = 11.5 \times 10^{10}\ \mathrm{N/m^2}$$

$$c_{33} = 2.56 \times 10^{10}\ \mathrm{N/m^2}$$

$$e_{12} = -5.2\ \mathrm{C/m^2}$$

$$e_{22} = 15.1\ \mathrm{C/m^2}$$

$$e_{31} = 12.7\ \mathrm{C/m^2}$$

$$\epsilon_{11} = 6.45 \times 10^{-9}\ \mathrm{C/Vm}$$

$$\epsilon_{22} = 5.62 \times 10^{-9}\ \mathrm{C/Vm}$$

6.1. Solution techniques

An iteration process has been used to solve the nonlinear Eq. (36), which can be expressed as,

$$\sum_{m=1}^{M} \mathbf{C}_m^{l(n+1)} \frac{\sin\left(m\cos^{-1}\frac{x_l}{a_l}\right)}{\sin\left(\cos^{-1}\frac{x_l}{a_l}\right)} + \sum_{k\neq l}^{N}\sum_{m=1}^{M} \int_{-a_k}^{a_k} (\mathbf{B}_1 + \mathbf{B}_2)\mathbf{C}_m^{k(n)} T_m\left(\frac{\xi}{a_k}\right) \Bigg/ \sqrt{1-\left(\frac{\xi}{a_k}\right)^2}\,\mathrm{d}\xi - \sum_{m=1}^{M} \mathbf{M}^{l(n)}\mathbf{C}_m^{l(n)} \frac{a_l}{m} \sin\left(m\cos^{-1}\frac{x_l}{a_l}\right) = -\mathbf{t}^0 \quad (l = 1,2,\ldots,N) \tag{43}$$

Numerical simulation indicates that the solution of Eq. (43) is not unique, i.e. two solutions corresponding to positive opening and negative opening (overlapping) for each crack can be obtained. For the case where two cracks are involved, four different modes can be predicted, i.e. both cracks are open; the first open and the second overlapping; the first overlapping and the second open; both overlapping. More complicated deformation modes can be observed when more cracks are involved. i.e. for N cracks, 2^N solutions exist. An overlapping crack may indicate the closure of the crack. For the current parallel crack problem, however, it is believed that a closed crack is physically impossible. This is because as soon as a crack is closed, the electric potential will be continuous across the crack surfaces. As the result, electric field will have no effect on this crack, and the applied tensile stress perpendicular to the crack will result in a crack opening. With this in mind, only the open-crack mode is considered in the current discussion.

To clearly identify the open-crack mode, a simplified solution is developed considering only one term in the Chebyshev polynomial expansion of the electric displacement $\mathbf{C}_{41}^l$ in Eq. (43), while M terms of c_{1j}^l, c_{2j}^l, c_{3j}^l, $(j = 1,2,\ldots,M)$, are still used. This treatment enables the determination of different response modes

analytically. In this case, M collocation points along the surfaces of each crack are used for the mechanical boundary conditions, however, only the central point is used for electric boundary condition. The solution of $\mathbf{C}_{41}^{l}$ corresponding to an open crack can be determined directly from Eq. (43).

The accuracy of the single-term solution mentioned above is verified by considering the interaction of two parallel cracks of the same length ($2a = 2$ mm), shown in Fig. 2, subjected to applied electromechanical loads σ_{22}^{∞} and D_2^{∞}, for the case where the distance between the cracks is $1.0a$. Fig. 2(a) shows the comparison between the maximum crack opening at the centre of the crack determined by the single-term solution and that by the complete solution obtained from Eq. (43) using 13 terms in the Chebyshev polynomial expansion. Fig. 2(b) shows the corresponding comparison between the stress intensity factors at the right tip of the crack determined by single-term and complete solutions. Good agreement between the two solutions

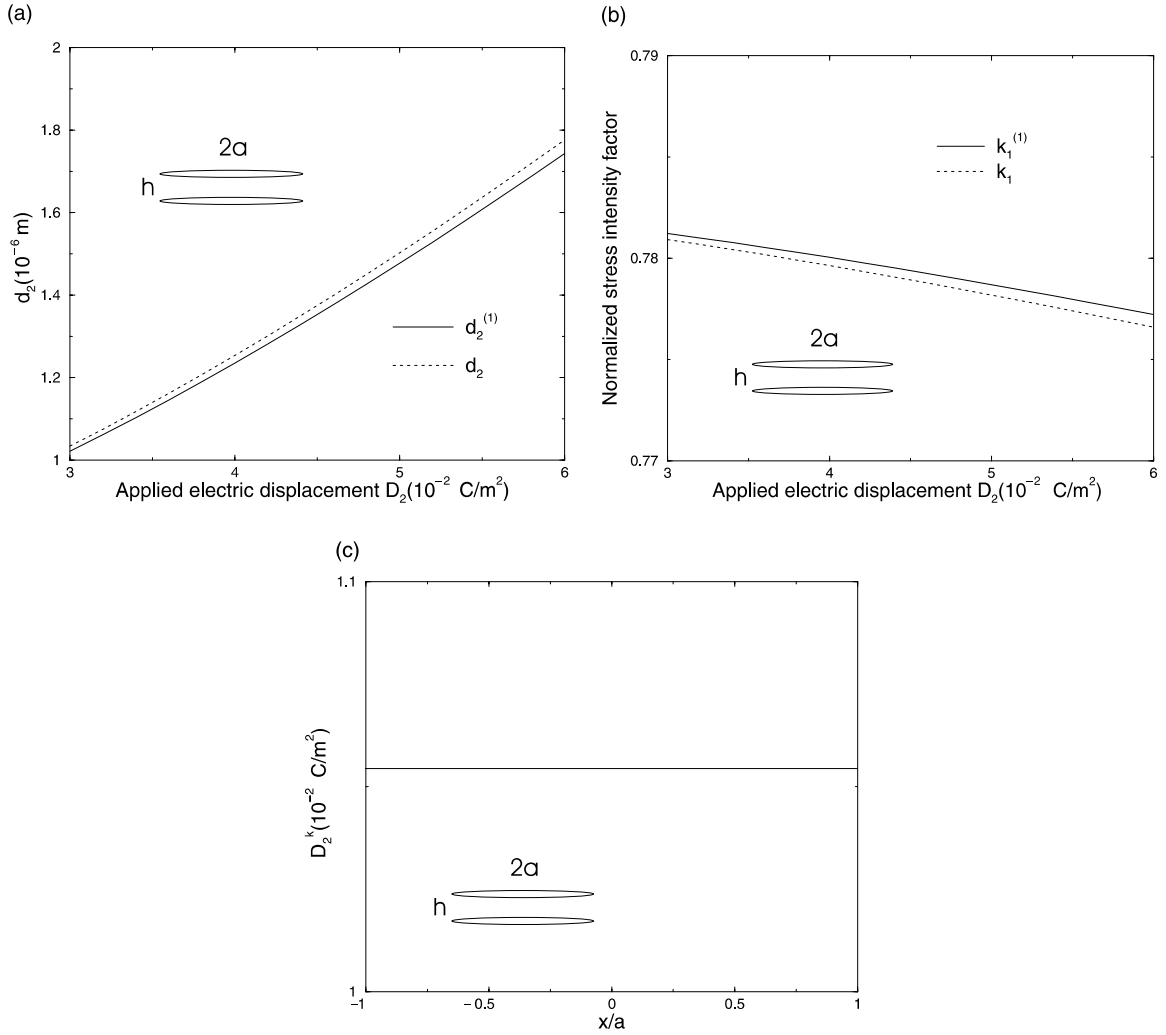

Fig. 2. (a) The maximum crack opening of two parallel cracks ($h = 1.0a$), (b) the normalized stress intensity factor at the right tip of one crack in two parallel crack problem ($h = 1.0a$), (c) the electric displacement distribution along the crack surface for two parallel crack problem ($h = 1.0a$).

can be observed. The variation of $\overline{D}_2^k$ along the crack surface obtained by the complete solution is depicted in Fig. 2(c), showing that $\overline{D}_2^k$ keeps almost constant. It is interesting to mention that a constant $\overline{D}_2^k$ distribution along the crack surface can be predicted by the first term of the Chebyshev polynomial expansion. Based on these results, the single-term solution will be used in the following discussion.

In this section, the interacting effect between the parallel cracks is represented by the traditional stress intensity factors, electric displacement intensity factor, COD intensity factor and energy release rate. The effect of electric boundary conditions upon the fracture property of piezoelectric materials is also described for different cases.

6.2. Interaction effect

The interaction between three equally spaced parallel cracks of the same size ($2a = 2$ mm) is studied. The system is subjected to a remote electromechanical loading $\sigma_{22}^{\infty} = 20$ MPa and $D_2^{\infty} = 0.001$ C/m^2. Fig. 3 shows the normalized stress intensity factors $k_{\mathrm{I}} = K_{\mathrm{I}}/K_{\mathrm{I}}^S$, $k_{\mathrm{II}} = K_{\mathrm{II}}/K_{\mathrm{I}}^S$ (with superscript S representing the corresponding intensity factors of one crack problem) for three cracks for different distance h between the adjacent cracks. The shielding effect on stress intensity factor K_{I} exists for these cracks, e.g. all normalized intensity factors k_{I} are less than 1, which is similar to that in traditional materials. K_{II} can be observed due to the interaction. The normalized stress intensity factor $k_{\mathrm{II}}(1)$ is approximately 25% of $k_{\mathrm{I}}(1)$ when the distance between the cracks is $0.4a$.

Fig. 4 shows the normalized electric displacement intensity factor $k_D = K_D/K_D^S$ for two parallel cracks of the same size ($2a = 2$ mm) under an electromechanical loading $\sigma_{22}^{\infty} = 20$ MPa and $D_2^{\infty} = 0.001$ C/m^2. The corresponding results k_D^{P} for electrically permeable cracks and k_D^{I} for electrically impermeable cracks are also given to show the coupled effect of boundary conditions and crack interaction. Changes of the shielding effect with different electric boundary conditions can be observed. For materials with weak piezoelectric effect, it is found that the shielding effect upon k_D for permeable, impermeable and the current models are significantly different.

The stress intensity factors of two parallel cracks of different sizes $2a_1$ ($a_1 = 1$ mm) and $2a_2$, normalized by the corresponding single crack solutions, are depicted in Fig. 5. The distance between the cracks is

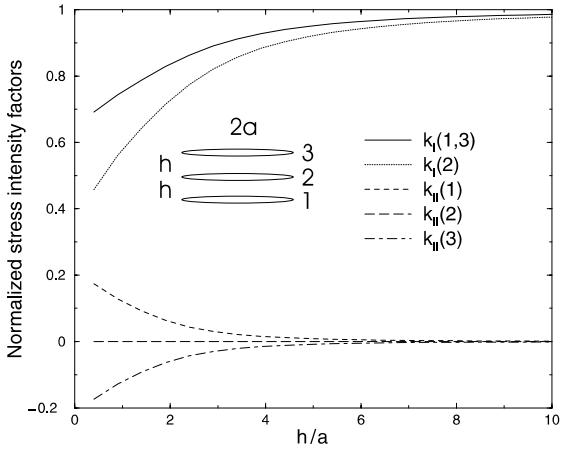

Fig. 3. The normalized stress intensity factors of interacting cracks.

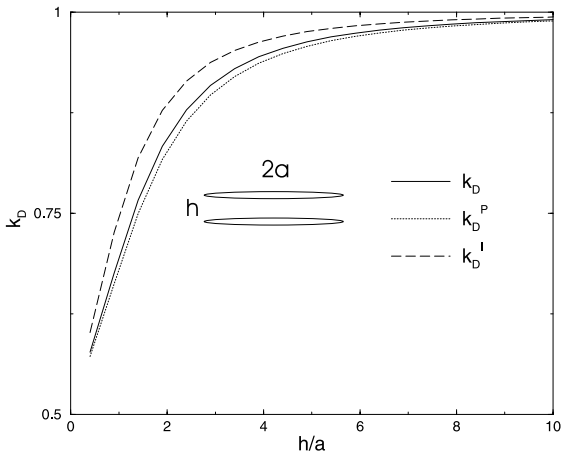

Fig. 4. The normalized electric displacement intensity factor in two parallel crack problem.

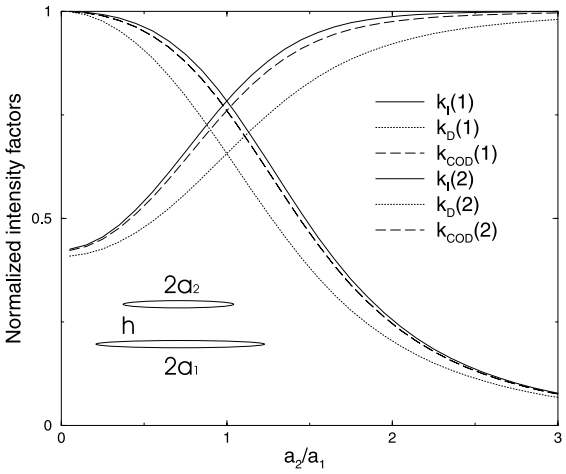

Fig. 5. The normalized intensity factors of interacting cracks ($h = a_1$).

assumed to be a_1 and the cracks are centrally aligned. With the increase of the length of the second crack a_2, the shielding effect on the first crack increases, but the effect on the second crack decreases.

6.3. Effects of the electric boundary condition

Another important issue in determining the fracture property of the cracked piezoelectric medium is the electric boundary condition. Fig. 6 shows the energy release rate of one of the two parallel cracks as depicted in Fig. 4 subjected to $\sigma_{22}^{\infty} = 20$ MPa. The distance between the cracks is assumed to be a. The resulting energy release rate G is bounded by G^{I} and G^{P} for the applied electric field considered, with G^{I} and G^{P} corresponding to the electrically impermeable and permeable boundary conditions along the crack

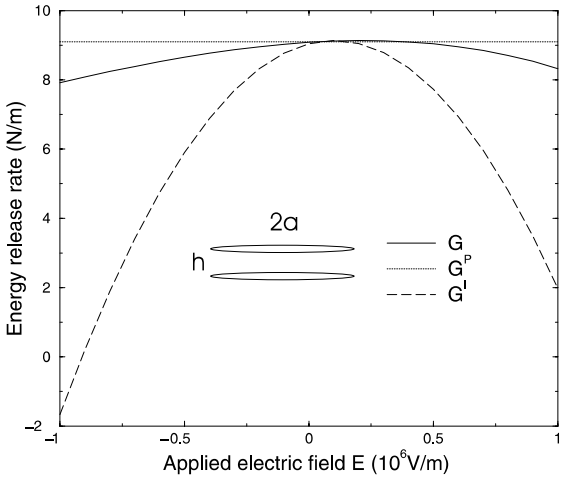

Fig. 6. Energy release rate of one crack in two parallel crack problem ($h = a$).

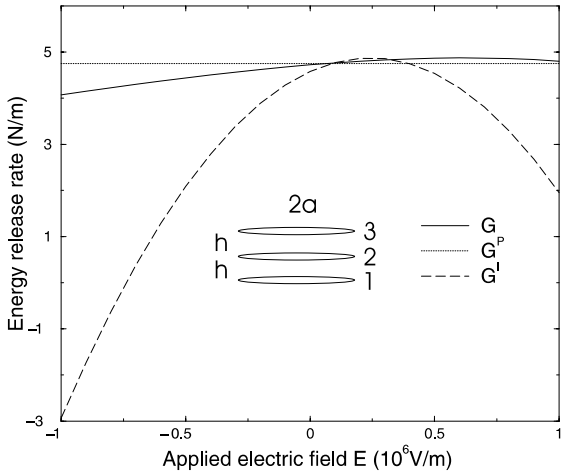

Fig. 7. Energy release rate of the central crack in three parallel crack problem ($h = a$).

surfaces. Fig. 7 shows the corresponding results for the central crack of three equally spaced parallel cracks as that in Fig. 3. It can be observed that neither G^{I} nor G^{P} can be used to provide a reasonable prediction of the energy release rate.

To describe the mechanical deformation, COD intensity factor K_{COD} in Eq. (42) is studied. Figs. 8 and 9 show the variation of K_{COD} with applied electric field intensity E_2^{∞} for the parallel crack problems studied in Figs. 4 and 3 subjected to $\sigma_{22}^{\infty} = 20$ MPa, with the distance between the adjacent cracks being a. The corresponding results $K_{\mathrm{COD}}^{\mathrm{I}}$ and $K_{\mathrm{COD}}^{\mathrm{P}}$ using electrically impermeable and permeable crack models are also provided in these figures for comparison. It can be observed that K_{COD} increases monotonically with increasing electric field. Significant difference between the results from impermeable, permeable and current crack models can be observed, indicating the necessity of considering the effect of the dielectric medium inside the crack. It is interesting to mention that if K_{COD} is used as a fracture parameter, it can be predicted

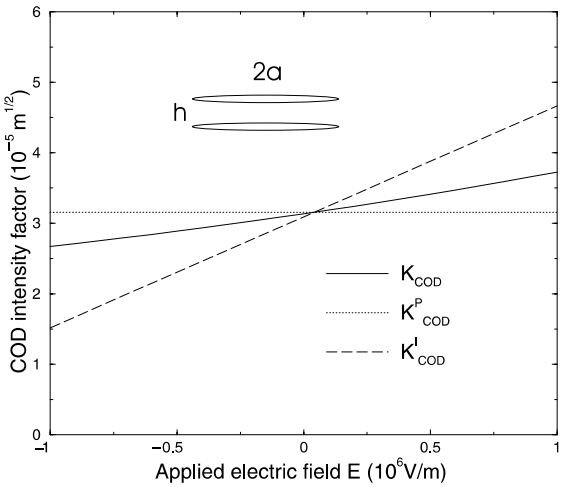

Fig. 8. COD intensity factor of one crack in two parallel crack problem ($h = a$).

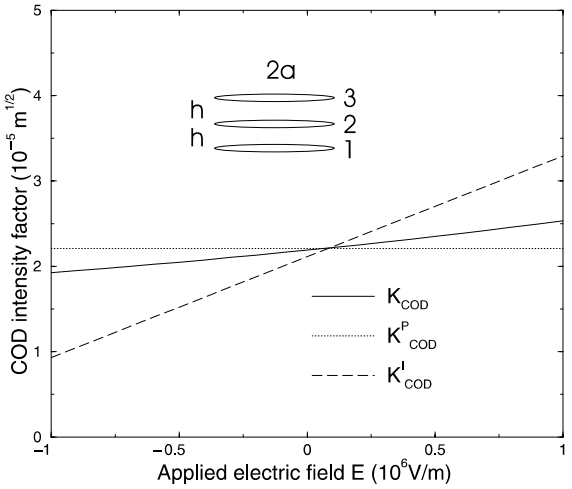

Fig. 9. COD intensity factor of the central crack in three parallel crack problem ($h = a$).

that the crack propagation can be either enhanced or impeded depending on the direction of the applied electric field as predicted by Park and Sun (1995) using strain energy release rate as the fracture criterion.

Fig. 10 shows the result of K_{COD} of one of the two parallel cracks as discussed in Fig. 8 for different applied tensile stress σ_{22}^{∞}, for the case where the applied electric field intensity is $E = 500$ V/mm. It shows that K_{COD} for the current model is between K^{I}_{COD} (impermeable model) and K^{P}_{COD} (permeable model), and is closer to the result of the electrically permeable model when the stress level is low, but closer to that of the electrically impermeable model with the increase of the stress level. The corresponding electric displacement intensity factor K_D is given in Fig. 11 for the case discussed in Fig. 10. Similar to K_{COD}, K_D approaches permeable and impermeable models for low and high tensile stress levels, respectively. This is because higher stress level will result in larger crack opening and therefore create an 'impermeable' crack. This

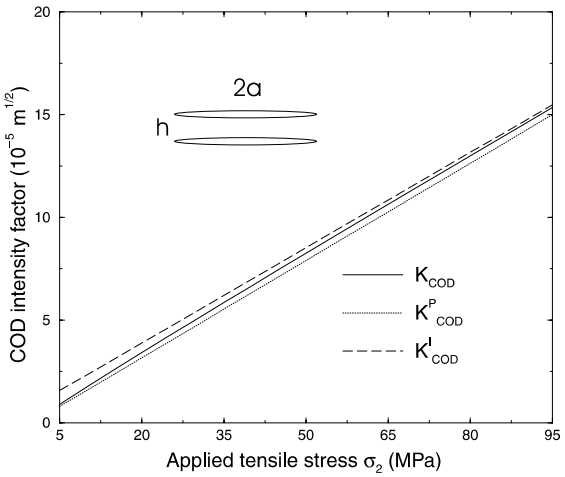

Fig. 10. COD intensity factor for two parallel crack problem subjected to an electric field ($h = a$).

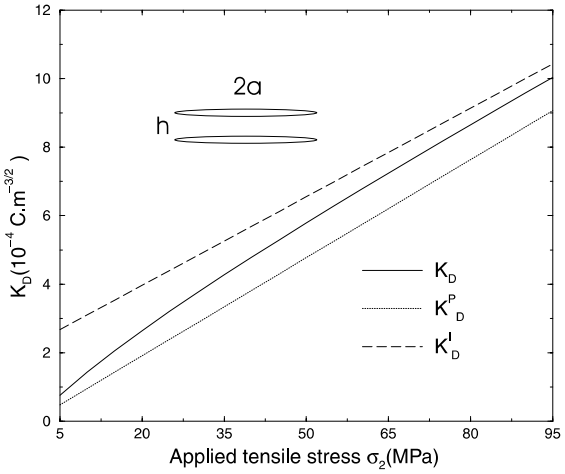

Fig. 11. Electric displacement intensity factor for two parallel crack problem subjected to an electric field ($h = a$).

phenomenon indicates the transition between the electrically permeable and impermeable models with the increase of the crack opening.

7. Conclusions

A theoretical study is provided to the plane problem of an infinite piezoelectric medium with multiple parallel dielectric cracks. The deformed crack geometry is used for formulating the nonlinear electric boundary condition. Attention is focused on the effects of the interaction between cracks and the loading dependent boundary condition on the fracture property. In addition to the well-known shielding effect for multiple crack problems, the current study indicates that the commonly used permeable and impermeable

crack models represent two limiting cases which may not be suitable for predicting the fracture behaviour of cracked piezoelectric medium in some cases.

Acknowledgements

This work was supported by the Natural Sciences and Engineering Research Council of Canada.

References

Chen, Y.H., Han, J.J., 1999a. Macrocrack–microcrack interaction in piezoelectric materials, part I: basic formulations and J-analysis. Journal of Applied Mechanics 66, 514–521.

Chen, Y.H., Han, J.J., 1999b. Macrocrack–microcrack interaction in piezoelectric materials, part II: numerical results and discussions. Journal of Applied Mechanics 66, 522–527.

Chen, Y.H., Hasebe, N., 1994. Interaction between a main crack and a parallel microcrack in an orthotropic plane elastic solid. International Journal of Solids and Structures 31, 1877–1890.

Chudnovsky, A., Dolgopolsky, A., Kachanov, M., 1987. Elastic interaction of a crack with a microcrack array part I and part II. International Journal of Solids and Structures 23, 1–21.

Deeg, W.E.F., 1980. The analysis of dislocation, crack, and inclusion problems in piezoelectric solids. Ph.D. thesis, Stanford University.

Dunn, M.L., 1994. The effects of crack face boundary conditions on the fracture mechanics of piezoelectric solids. Engineering Fracture Mechanics 48, 25–39.

Gong, S.X., Meguid, S., 1991. On the effect of the release of residual stress due to near-tip microcracking. International Journal of Fracture 52, 257–274.

Han, X.L., Wang, Z.C., 1999. Interacting multiple cracks in piezoelectric materials. International Journal of Solids and Structures 36, 4183–4202.

McHenry, K.D., Koepke, B.G., 1983. Electric field effects on subcritical growth in PZT. Fracture Mechanics of Ceramics 5, 337–352.

McMeeking, R.M., 1989. Electrostrictive stresses near crack-like flaws. Journal of Applied Mathematics and Physics 40, 615–627.

Meguid, S.A., Wang, X.D., 1995. On the dynamic interaction between a microdefect and a main crack. Proceedings of Royal Society of London A448, 449–464.

Pak, Y.E., 1992. Linear electro-elastic fracture mechanics of piezoelectric materials. International Journal of Fracture 54, 79–100.

Pak, Y.E., 1990. Crack extension force in a piezoelectrical material. Journal of Applied Mechanics 57, 647–653.

Park, S., Sun, C.T., 1995. Fracture criteria for piezoelectric ceramics. Journal of American Ceramic Society 78, 1475–1480.

Parton, V.Z., 1976. Fracture mechanics of piezoelectric materials. Acta Astronaut 3, 671–683.

Rubinstein, A.A., 1986. Macrocrack–microdefect interaction. ASME Journal of Applied Mechanics 53, 505–510.

Sosa, H., 1991. Plane problems in piezoelectric media with defects. International Journal of Solids and Structures 28, 491–505.

Suo, Z., Kuo, C.M., Barnett, D.M., Willis, J.R., 1992. Fracture mechanics for piezoelectric ceramics. Journal of Mechanics and Physics of Solids 40, 739–765.

Tobin, A.G., Pak, Y.E., 1993. Effect of electric fields on fracture behavior of PZT ceramics. SPIE 1916, 78–86.

Wang, X.D., 2000. On the dynamic behavior of interacting interfacial cracks in piezoelectric media. International Journal of Solids and Structures, in press.

Zhang, T.Y., Tong, P., 1996. Fracture mechanics for a mode-III crack in a piezoelectric material. International Journal of Solids and Structures 33, 343–359.

Zhang, T.Y., Qian, C.F., Tong, P., 1998. Linear electro-elastic analysis of a cavity or a crack in a piezoelectric material. International Journal of Solids and Structures 35 (17), 2121–2149.